Compensation of Dispersion and Nonlinear Impairments Using Digital Backpropagation

Ezra Ip and Joseph M. Kahn, *Fellow, IEEE*

Abstract—**Optical fiber transmission is impacted by linear and nonlinear impairments. We study the use of digital backpropagation (BP) in conjunction with coherent detection to jointly mitigate dispersion and fiber nonlinearity. We propose a noniterative asymmetric split-step Fourier method (SSFM) for solving the inverse nonlinear Schrödinger equation (NLSE). Using simulation results for RZ-QPSK transmitted over terrestrial systems with inline amplification and dispersion compensation, we obtain heuristics for the step size and sampling rate requirements, as well as the optimal dispersion map.**

Index Terms—**Coherent detection, chromatic dispersion, digital signal processing, optical communications, optical Kerr effect, phase noise, phase shift keying.**

I. INTRODUCTION

TRANSMISSION impairments in optical fiber can be divided into two categories: linear impairments, which include chromatic dispersion (CD), polarization-mode dispersion (PMD), symbol timing offset, and optical filtering; and nonlinear impairments, which include laser phase noise, self-phase modulation (SPM), cross-phase modulation (XPM), four-wave mixing (FWM), and nonlinear phase noise (NLPN). Until recently, compensation techniques for different impairments have been considered separately. Digital equalization of linear impairments using a fractionally spaced finite impulse response (FIR) filter was studied in [1]–[3], while digital feedforward carrier recovery to overcome laser phase noise was studied in [4]–[7]. XPM has traditionally been mitigated using nonzero-dispersion fiber to induce pulse walkoff [8]. Techniques for reducing the impact of NLPN have included transmitter-based electronic precompensation [9], optical phase conjugation [10]–[12] and receiver-based electronic phase rotation [13].

Recently, backpropagation (BP) was proposed as a universal technique for jointly compensating linear and nonlinear impairments [14], [15]. BP involves solving an inverse nonlinear Schrödinger equation (NLSE) through the fiber to estimate the transmitted signal. BP has been shown to enable
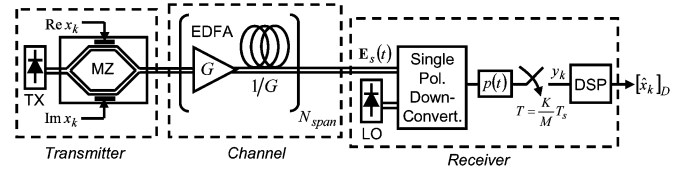
Fig. 1. Canonical zero-dispersion long-haul system employing inline amplification.

higher launched power and longer system reach in dense wavelength-division-multiplexed (WDM) transmission over zero-dispersion fiber [14]. The main drawbacks of BP are its excessive computational requirement and the difficulty in applying it in the presence of PMD. In this paper, we introduce a computationally simpler algorithm for solving the NLSE based on a noniterative asymmetric split-step Fourier method (SSFM).

The structure of this paper is as follows. In Section II, we review receiver-based electronic phase rotation, which has been shown to reduce NLPN for certain optimized channels [16], [17]. Our numerical simulations show that this technique fails for general terrestrial systems employing inline amplification and dispersion compensation where there is moderate CD undercompensation per span. In Section III, we review digital BP and propose a computationally simpler approach to solving the NLSE. We compare the performance and computation requirements of BP with other receiver-based algorithms. We evaluate the performance of BP for different dispersion maps, step size settings and sampling rate requirement to obtain heuristics for system design. We will also consider the application of BP to WDM systems.

II. NONLINEAR COMPENSATION

Consider the canonical coherent optical system shown in Fig. 1 which employs digital signal processing at the receiver for impairment compensation. The channel consists of N_{span} of zero-dispersion fiber, where the gain G of each inline erbium-doped fiber amplifier (EDFA) exactly equals the loss of each fiber span. In the absence of CD and PMD, the nonlinear phase shift experienced by the received signal is [13]

$$\phi_{NL,n} = \gamma L_{\text{eff}} \sum_{k=1}^{N_{\text{span}}} \left| x_n + \sum_{l=1}^{k} m_{l,n} \right|^2 \qquad (1)$$

where γ and L_{eff} are the nonlinear parameter and effective length of the fiber, x_n is the nth transmitted symbol, and $m_{l,n}$ is the amplified spontaneous emission (ASE) noise of the lth amplifier, which is an additive white Gaussian noise process (AWGN) with zero mean and variance $E[|m_{l,n}|^2] = 2\sigma^2$. The
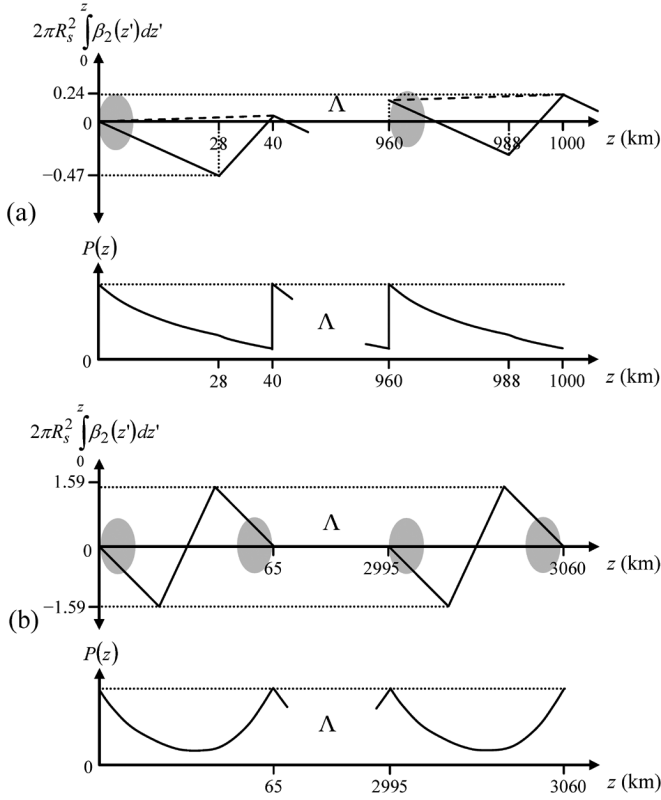
Fig. 2. Dispersion map and power profile for the experimental setups used by: (a) Kikuchi *et al.* [16]; and (b) Charlet *et al.* [17].
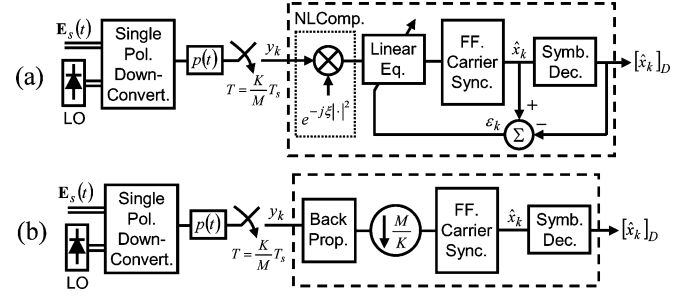

Fig. 3. Integrated digital coherent receivers for single-polarization transmission, integrating the functions of downconversion and channel impairment compensation. These receivers show nonlinear compensation using: (a) amplitude-dependent phase rotation; and (b) digital BP.

received signal $y_n = x_n \exp(j\phi_{NL,n})$ has a spiral-shaped constellation [18]. It is possible to exploit the correlation between the received amplitude and NL phase shift to reduce NLPN variance. A simple compensation scheme is

$$\hat{\phi}_n = \psi_n - \xi|y_n|^2 \tag{2}$$

where $\psi_n = \arg y_n$ is the phase of the received signal, ξ is a coefficient to be optimized, and $\hat{\phi}_n$ is the corrected phase. [13] showed that the optimum value of ξ is

$$\xi_{opt} \approx -\gamma L_{\text{eff}}(N_{\text{span}} + 1)/2 \tag{3}$$

which corresponds (in a mean sense) to derotating the received signal by half the mean nonlinear phase shift $\langle \phi_{NL_n} \rangle$. It has been shown that this NLPN compensation scheme reduces NLPN variance by four: $\sigma_{\hat{\phi}_n}^2 \approx (1/4)\sigma_{\psi_n}^2$.

The ability of amplitude-dependent phase rotation to improve system performance has been demonstrated in [16] and [17]. In both experiments, short fiber spans were used with nearly perfect CD compensation per span. Fig. 2 shows the approximate dispersion maps and power profiles used by the two experiments. It is observed that the local dispersion at any point in the link is small, and peak power occurs when the accumulated dispersion is nearly zero, $2\pi R_s^2 \int_0^z \beta_2(z')dz' \approx 0$. Since fiber nonlinearity has greatest effect at high power, in a first-order approximation where we assume nonlinear effects are localized at the points of peak power, (1) is a good model of NL phase. Consequently, the phase rotation algorithm is successful at reducing the NLPN variance.

The results of [16] and [17] suggests an integrated receiver shown in Fig. 3(a) [19]. A single-polarization optoelectronic downconverter recovers the analog inphase and quadrature components of the optical E-field. Its output is passed through an antialiasing filter $p(t)$ and then synchronously sampled at a rate $1/T = M/KT_s$ where T_s is the symbol period and M/K is an integer fraction oversampling ratio. NLPN compensation is performed first, as (2) requires only the received amplitudes at the sampling instants. The derotated signal is then passed through a fractionally spaced linear equalizer whose output is one sample per symbol. Feedforward carrier recovery follows.

We simulated the performance of the receiver of Fig. 3(a) for 21.4 Gb/s 50% RZ-QPSK[1] over the transmission system shown in Fig. 4(a). We select this transmission model as it is representative of long haul terrestrial systems with inline amplification and dispersion compensation. The parameters of the link components used are shown in Table I. We assume the two EDFAs have equal gain that exactly compensate the signal attenuation by the SMF and DCF. We undercompensate CD by 10% per span. At the receiver, no tunable dispersion compensation is used. Instead, residual CD is compensated using the fractionally spaced linear equalizer shown in Fig. 3(a), whose coefficient are set in accordance with [2]. The antialiasing filter $p(t)$ is a fifth-order Butterworth filter whose 3-dB cutoff frequency is 40% of the sampling rate. In all simulations considered in this paper, we neglect laser phase noise, focusing only on *fiber* impairments. Feedforward carrier recovery is then reduced to a constant phase rotation.

Fig. 5 shows the performance obtained for the integrated receiver with and without the NLPN compensator, while the dotted curve is the theoretical AWGN limit of $\sigma_\varepsilon^2 = 1/2$SNR. At low launched power, both systems have similar performances that approach the AWGN limit. At higher launched powers, nonlinear effects cause excess phase error variance. In contrast with the results of [16] and [17], the NLPN compensator does not improve system performance. In fact, worse results were obtained compared to linear equalization only. Fig. 6(a) and (b) shows the equalized constellations $(\hat{x}_k)$ for the two algorithms when the launched power is 2 dBm. The NLPN compensator fails because there are significant nonlinear effects occurring at the start of each span of DCF, where

[1]We assume a raw information rate of 20 Gb/s with 7% overhead for Reed-Solomon coding.
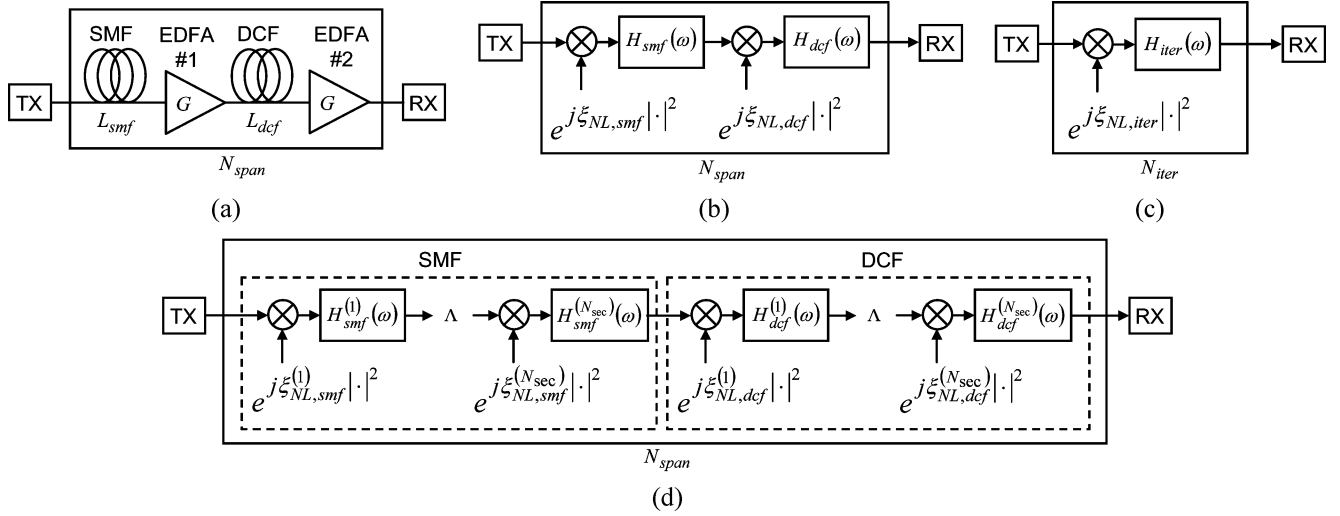
Fig. 4. (a) Canonical model of a long-haul terrestrial link with inline amplification and dispersion compensation. The propagation effects are modeled as the concatenation of nonlinear phase rotations and linear dispersion sections. The mathematical models shown here are for: (b) BP with span-length step size (BP-1S); (c) BP with multispan step size (BP-MS); and (d) BP with subspan step size (BP-SS).

TABLE I
FIBER AND EDFA PARAMETERS FOR A HYPOTHETICAL TERRESTRIAL LINK

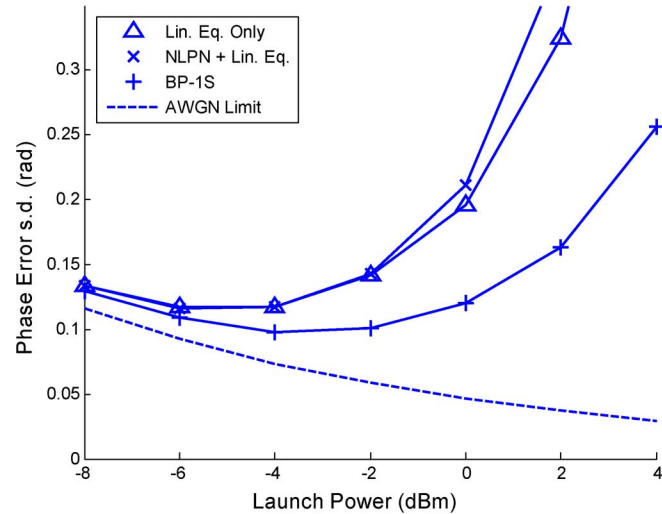| SMF	DCF	EDFA
α_{SMF} = 0.2 dB/km	α_{DCF} = 0.6 dB/km	$G_{(dB)} = \frac{1}{2}\left(\begin{array}{c}\alpha_{SMF}L_{SMF} + \\ \alpha_{DCF}L_{DCF}\end{array}\right)$
D_{SMF} = 17 ps/nm/km	D_{DCF} = −80 ps/nm/km	
γ_{SMF} = 0.013 m^{-1}W^{-1}	γ_{DCF} = 0.053 m^{-1}W^{-1}	
L_{SMF} = 80 km	L_{DCF} = 15.3 km	NF = 5 dB

Fig. 5. Comparison of the performances of different algorithms for combatting CD + linearity for 21.4 Gb/s 50% RZ-QPSK transmitted over 25 × 80 km spans of SMF with 10% CD undecompensation per span. An oversampling rate of $M/K = 2$ was used.

the accumulated dispersion is nonnegligible. Equation (1) is, therefore, an inadequate model of NL phase, causing the phase rotation algorithm to fail.

III. BACKPROPAGATION

A. Split-Step Fourier Method (SSFM)

Signal propagation in fiber is described by the nonlinear Schrödinger equation (NLSE):[2]

$$\frac{\partial E}{\partial z} = (\hat{N} + \hat{D})E \qquad (4)$$

$$\hat{N} = j\gamma|E|^2 \qquad (5)$$

$$\hat{D} = -j\frac{\beta_2}{2}\frac{\partial^2}{\partial t^2} - \frac{\alpha}{2} \qquad (6)$$

where $\hat{D}$ and $\hat{N}$ are the linear and nonlinear operators, and α, β_2, and γ are the attenuation, CD, and nonlinear coefficients of the fiber. In the absence of noise, the transmitted signal can be calculated from the inverse NLSE: $\partial E/\partial z = (\hat{N}^{-1} + \hat{D}^{-1})E$, which is equivalent to passing the received signal through a fiber with parameters of the opposite sign. The NLSE can be solved numerically using the symmetric split-step Fourier method (SSFM) [14], [20]

$$E(z + h, t) = \exp\left(\frac{h}{2}\hat{D}\right)\exp\left(\int_z^{z+h}\hat{N}(z')dz'\right)$$
$$\times \exp\left(\frac{h}{2}\hat{D}\right)E(z, t) \quad (7)$$

where h is the step size. Since the nonlinear operator depends on E itself, the integral for $\hat{N}(z)$ is usually approximated by the trapezoidal rule, and an iterative procedure is used to solve (7) [14]. The accuracy of iterative symmetric SSFM improves with

[2]The use of a scalar NLSE is valid when polarization-mode dispersion (PMD) is negligible, which is true for 20 Gb/s systems over SMF at distances up to several thousand kilometers [2]. The only polarization effect is a frequency-independent rotation between the input and output states of polarizations. Signal propagation is then described by a scalar NLSE in the reference polarization of interest, which can rotate throughout the link.
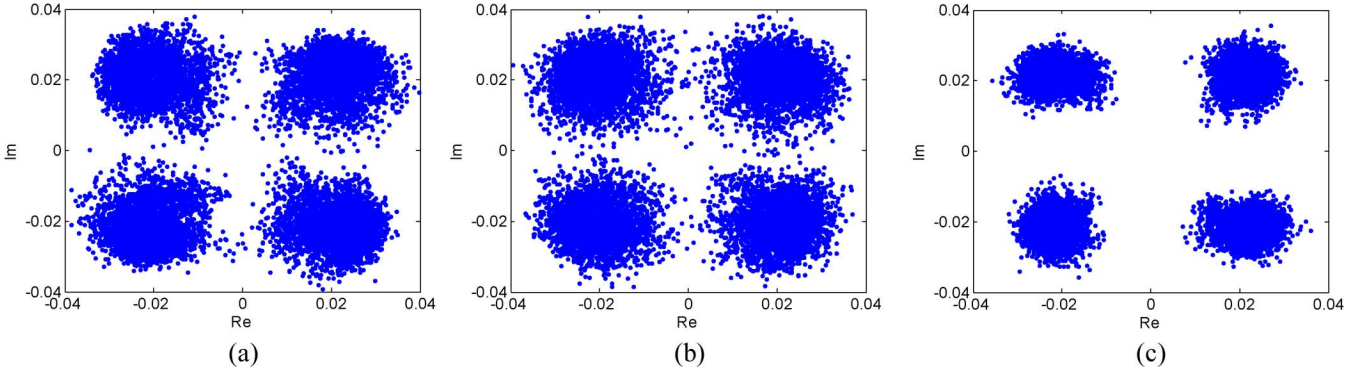
Fig. 6. Equalized constellations for 21.4 Gb/s 50% RZ-QPSK transmitted over 25×80 km spans of SMF with 10% CD undecompensation per span at 0 dBm launched power. The algorithms used are: (a) linear equalization only; (b) NLPN compensation + linear equalization; and (c) BP-1S.
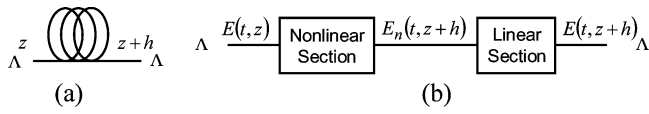

Fig. 7. (a) Fiber section from z to $z + h$. (b) Mathematical model.

```
for span = 1:Nspan
    y = ifft(fft(y).*conj(H_dcf));
    y = y .* exp(-jξ_dcf|y|²);
    y = ifft(fft(y).*conj(H_smf));
    y = y .* exp(-jξ_smf|y|²);
end;
```

Fig. 8. Matlab pseudocode for BP-1S.

increasing the number of iterations used to solve (7), and by decreasing the step size. Both of these increase the computational requirement.

In this paper, we use a computationally less expensive algorithm based on a noniterative asymmetric SSFM where the fiber is modeled as a concatenation of nonlinear and linear sections. Simplified BP has previously been considered for electronic precompensation in [21]. Consider Fig. 7, where

$$E_n(t, z + h) = E(t, z) \exp\left(j\gamma h \left| E(t, z) \right|^2 \right) \qquad (8)$$

and

$$\widetilde{E}(\omega, z + h) = \widetilde{E}_n(\omega, z + h)$$
$$\times \exp\left(-j \left(\frac{\alpha}{2} + \frac{\beta_2}{2}\omega^2 \right) h \right). \qquad (9)$$

We base this model on the heuristic that nonlinear effects are strongest at the beginning of a fiber section where signal power is highest. Thus, nonlinear phase rotation is performed first before linear propagation. In the limit of h being infinitesimally small, both the asymmetric SSFM and symmetric SSFM approach the true NLSE solution. We observe from (8) and (9) that fiber impairments are primarily two phase effects: CD is a phase multiplication in the frequency domain, whereas Kerr nonlinearity is a phase multiplication in the time domain. As both of these operations are invertible, the NLSE is also invertible.

The (symmetric) SSFM has been successfully employed for simulating the propagation of solitons. The step size requirement for modeling communication systems was studied in [22]. For signal detection however, it is not necessary to compute the NLSE to a high degree of accuracy: we merely need to make h small enough so that numerical errors are small compared to the impact of AWGN. In particular, ASE causes amplitude fluctuations so that the inversion of (8) results in derotation by a noisy phase proportional to $|E|^2$. When solving an NLSE with many sections, noise causes the BP solution to diverge from the true input signal. This effect occurs regardless of the step size used. In the remainder of this section, we propose three choices of step size for digital BP and compare their usefulness. A digital coherent receiver implementing BP is shown in Fig. (3b). Since BP corrects for both linear and nonlinear impairments, the adaptive linear equalizer can be replaced with a fixed downsampler.

B. Backpropagation With Span-Length Step Size (BP-1S)

In our first approximation, we make the step size equal to the length of a fiber span. The mathematical model of the channel is shown in Fig. (4b), where

$$H_{smf}(\omega) = \exp(-j\beta_{2,smf}L_{smf}\omega^2/2) \qquad (10)$$
$$H_{dcf}(\omega) = \exp(-j\beta_{2,dcf}L_{dcf}\omega^2/2) \qquad (11)$$
$$\xi_{NL,smf} = \xi\gamma_{smf}L_{\text{eff},smf} \qquad (12)$$
$$\xi_{NL,dcf} = \xi\gamma_{dcf}L_{\text{eff},dcf}Ge^{-\alpha_{smf}L_{smf}}. \qquad (13)$$

The parameter $0 < \xi < 1$ in (12) and (13) needs to be optimized empirically, and its value depends on the dispersion map, launched power, and rate of oversampling. In pure BP, $\xi = 1$ exactly inverts the nonlinear phase of the fiber, and is optimal in the limit of high SNR. For the particular case of zero dispersion fiber (Section II), the optimal value of ξ is 1/2.

We simulated the performance of BP-1S for 21.4 Gb/s 50% RZ-QPSK transmitted over the terrestrial channel considered in Section II. The input signal used is a random periodic sequence with a block length of 32 768 symbols. Fig. 8 shows the pseudocode for our BP-1S algorithm. The linear step of the SSFM is computed in the frequency domain using the fast Fourier transform (FFT). The long block length ensures almost perfect equalization of CD with negligible power penalty in the absence of Kerr nonlinearity, provided the oversampling rate is sufficiently
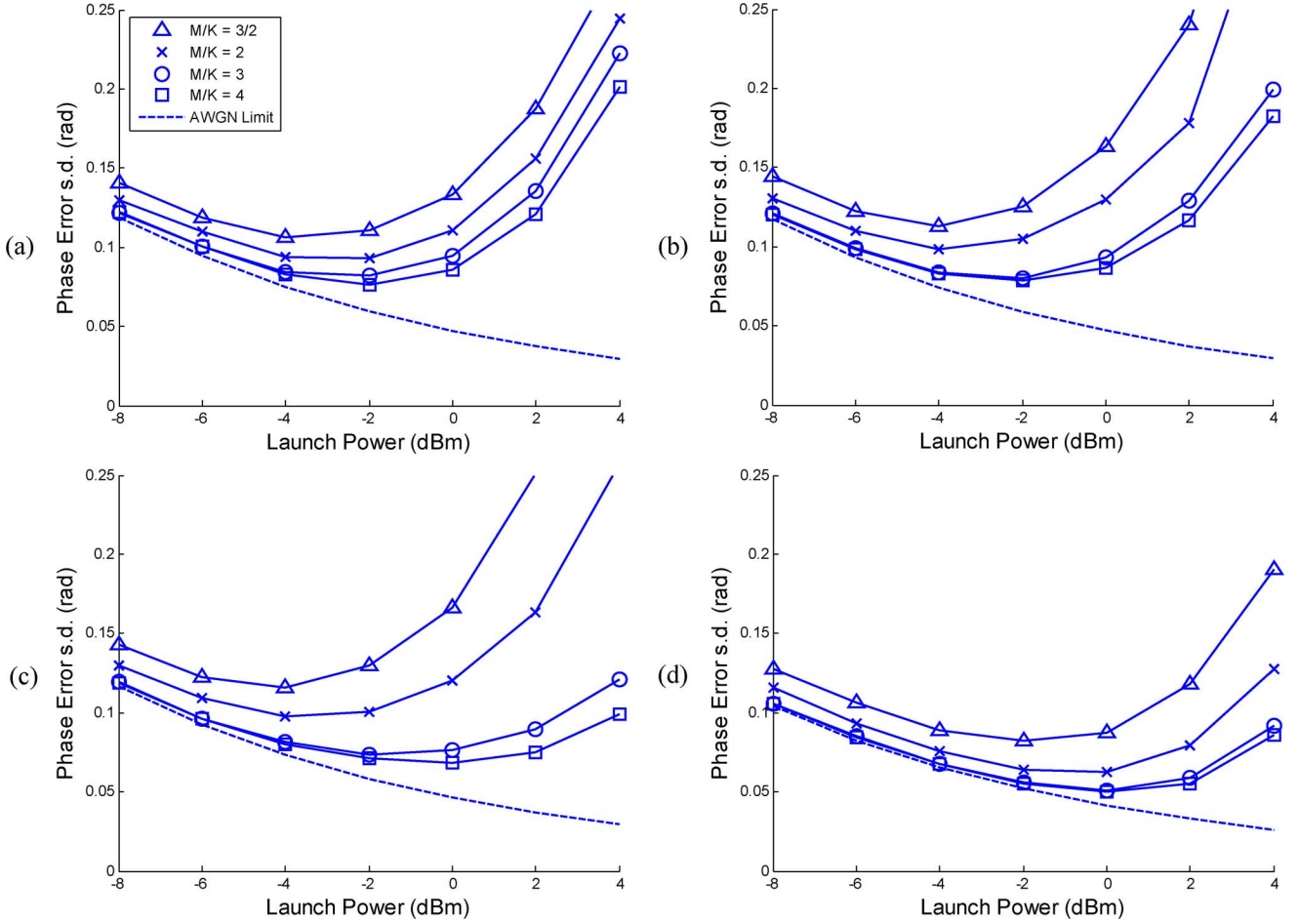
Fig. 9. Performance of BP-1S for 21.4 Gb/s 50% RZ-QPSK transmitted over 25 × 80 km spans of SMF. The CD undercompensation per span are: (a) 0%; (b) 5%; (c) 10%; and (d) 100%.

high. In practice, the linear step can be implemented with an FIR filter (see Section III-G).

The performance of BP-1S is shown in Fig. 5. In comparison with the algorithms considered in Section II, BP-1S yields significantly better performance at high powers. In order to determine how system performance varies with the dispersion map, we varied the amount of CD undercompensation per span by changing the length of the DCF while keeping the EDFA parameters the same as Table I. The results are shown in Fig. 9(a) to (d) for CD undercompensation of 0%, 5%, 10%, and 100% per span. Two key obvservations can be made from these results. First, system performance is improved by increasing the CD undercompensation per span. This is due to two factors: (i) dispersion causes noise to walk off from the signal, reducing nonlinear interactions between them; (ii) DCF incurs loss and nonlinear effects so it is better to compensate dispersion digitally. In practice, laser phase noise may limit the amount of tolerable uncompensated CD, since the received samples are modulated by a time-varying phase, making a long channel impulse response undesirable. However, many modern tunable lasers have linewidths <1 MHz. If a system uses a symbol rate of 10.7 GHz, $\Delta\nu T_s \approx 10^{-4}$. Since the channel impulse duration is approximately $N_{CD} = 2\pi N_{\text{span}}|\beta_{2,smf}L_{smf} - \beta_{2,dcf}L_{dcf}|R_s^2$ symbols, even with no DCF, N_{CD} is only 31 symbols for transmission over 25 × 80 km spans of SMF. Laser phase

noise is therefore not a major concern for realistic transmission distances.

The second key observation from Fig. 9 is that increasing the oversampling rate improves system performance, since digital BP becomes closer to analog BP. At 10% CD undercompensation per span, an oversampling rate of $M/K = 4$ enables the optimal launched power be increased from -2 dBm to $+2$ dBm compared to $M/K = 3/2$. The improvement in phase error s.d. from 0.095 to 0.0443 rad represents a 6.6 dB gain. We observe in Fig. 9(b) to (d) that most of the performance gain is obtained by increasing the oversampling rate M/K from 3/2 to 3, whereas there is only a small incremental improvement in raising M/K to 4. This indicates $M/K = 3$ may be a good compromise. The factor of three arises because the nonlinear term in the NLSE is third-order in E. This suggests BP may be susceptible to tight optical filtering. As optical networks have reconfigurable optical add-drop multiplexers (ROADMs), it is possible that the loss of high-frequency components that are created by nonlinearity will degrade the performance of BP. To test this, we inserted five ROADMs to the channel at equal intervals: one ROADM after each five transmission spans. We assume each ROADM has a transfer function given by a super-Gaussian:

$$H_{ROADM}(\omega) = \exp\left(-\ln 2\left(\frac{2\omega}{\omega_{1/2}}\right)^{2m}\right) \qquad (14)$$
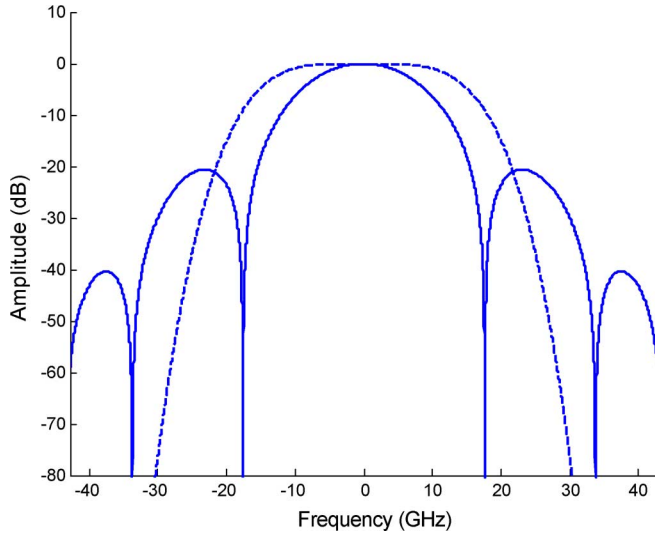
Fig. 10. Amplitude transfer function of five concatenated ROADMs (dotted curve), and the spectrum of 21.4 Gb/s 50% RZ-QPSK signal (solid curve).

where $\omega_{1/2}$ is the 3-dB bandwidth of the amplitude response of the device's the input and output ports. Fig. 10 shows the spectrum of a 21.4 Gb/s 50% RZ-QPSK signal superimposed over the amplitude response of a channel with five ROADMs where $m = 2$ and $\omega_{1/2} = 2\pi \cdot 40$ GHz.

The performance of BP-1S with the ROADMs inserted is shown in Fig. 11 when the undercompensation per span is 10%. There is no observe difference between these results and Fig. 9(c). We also performed simulations for 0%, 5%, and 100% CD undercompensation per span and obtained results indistinguishable from Fig. 9(a), (b), and (d). Since optical filtering apparently has no effect on performance, the oversampling requirement is due to the algorithm itself. Namely, the nonlinear phase rotations in lines 2 and 4 of Fig. 8 produce high frequencies. If BP is performed at an insufficient time resolution, aliasing results. When backpropagating through many fiber sections, the aliasing distortion accumulates, causing the discrete-time BP output to diverge from the ideal continuous-time BP output.

Using the heuristic design rule that the best system performance is obtained by omitting DCF, we simulated BP-1S for 21.4 Gb/s 50% RZ-QPSK for different transmission distances. The results are shown in Fig. 12(a) and (b) for $M/K = 2$ and 3, respectively. A launched power of 0 dBm was used. We compare the performances of BP-1S with iterative symmetric BP with 10 sections per span and two iterations per step (BP-SSFM10), which is the algorithm used in [14]. At $M/K = 2$, there is no observable difference in their performances, while at $M/K = 3$, BP-SSFM10 performs about 2 dB better, but has much higher computational requirement. We also performed simulation at $M/K = 4$, but the results are almost identical to $M/K = 3$. The gap between BP-SSFM10 and the theoretical AWGN limit is due to noise causing BP to divergence from the actual transmitted signal. Since QPSK requires $\sigma_\varepsilon < 0.23$ rad to achieve a BER of 10^{-3}, BP easily enables transmission over 6400 km of SMF. In contrast, a receiver implementing only linear equalization can transmit up to ∼2000 km only.
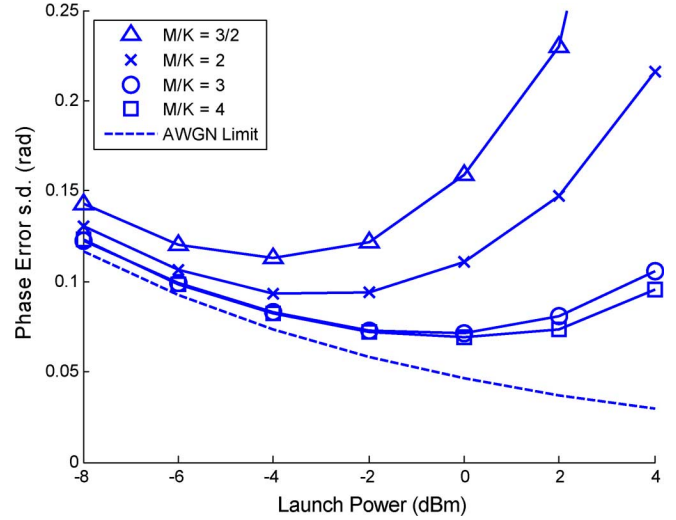

Fig. 11. Performance of BP-1S for 21.4 Gb/s 50% RZ-QPSK transmitted over 25×80 km spans of SMF with 5 ROADMs, with 10% CD undercompensation per span.
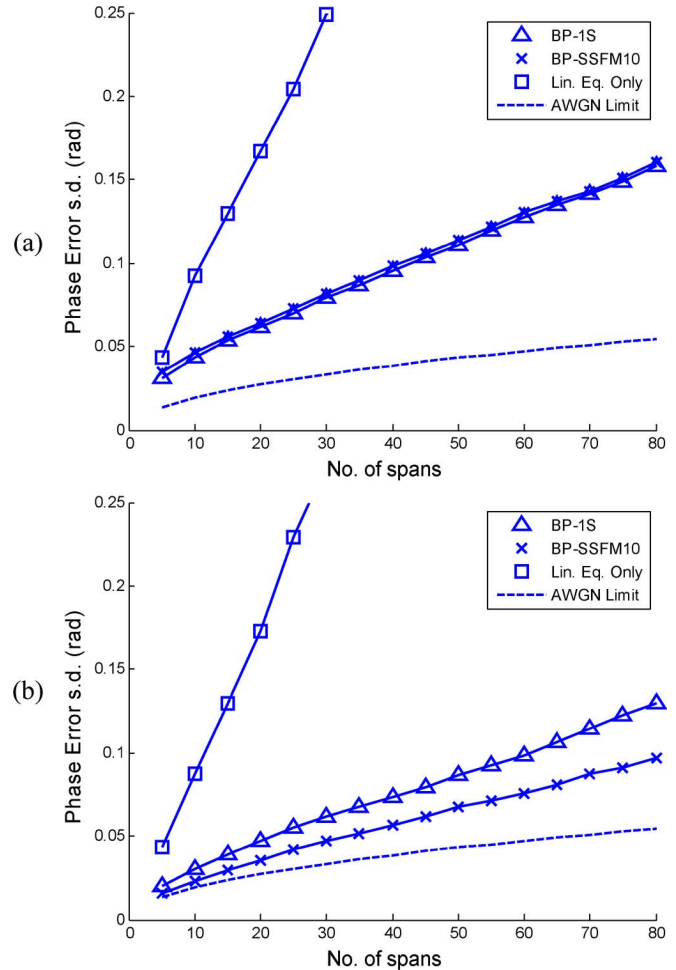

Fig. 12. System performance versus transmission distance for receivers implementing various algorithms for impairment compensation. The oversampling rates M/K are (a) 2 and (b) 3.

C. BP With Multispan Step Size

One of the drawbacks of BP-1S is that the receiver needs knowledge of the fiber parameters as well as the signal power level used. In our second approximation, we attempt to reduce
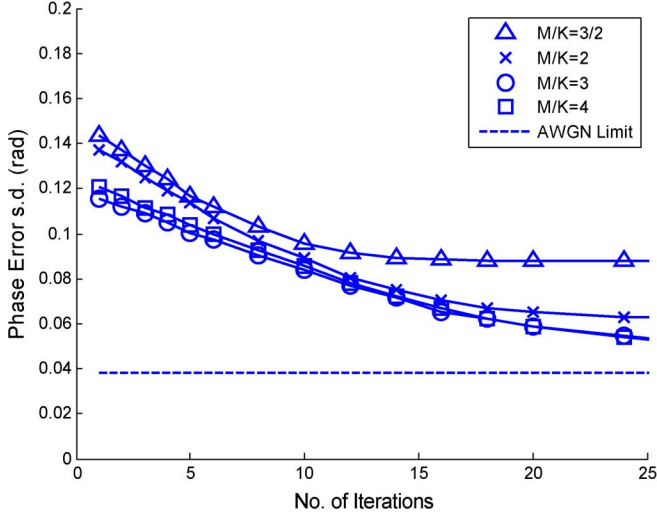
Fig. 13. Phase error s.d. versus N_{iter} for 50% RZ-QPSK at 21.4 Gb/s transmitted over 25×80 km spans of SMF with 10% CD undercompensation per span, detected using BP-MS. The dotted curve shows the AWGN limit.

Fig. 14. Performance of BP-1S for 53.5 Gb/s 50% RZ-QPSK transmitted over 25×80 km spans of SMF at 10% CD undercompensation per span.

the computational requirement further by using a multi-span step size. We model the channel as the concatenation of N_{iter} fictitious fiber sections shown in Fig. 4(c). In order that our fictitious link has the same uncompensated CD and nonlinear phase shift as the actual link, we set the linear and nonlinear operations to

$$H_{\text{iter}}(\omega) = \exp\left(-j\frac{N_{\text{span}}}{2N_{\text{iter}}}(\beta_{2,smf}L_{smf} \right.$$
$$\left. + \beta_{2,dcf}L_{dcf})\omega^2\right) \qquad (15)$$

$$\xi_{NL,\text{iter}} = \xi\frac{N_{\text{span}}}{N_{\text{iter}}}(\gamma_{smf}L_{\text{eff},smf}$$
$$+ \gamma_{dcf}L_{\text{eff},dcf}Ge^{-\alpha_{smf}L_{smf}}) \qquad (16)$$

where ξ is a parameter to be optimized empirically as in BP-1S. We simulated the performance of BP-MS for the channel considered in Section II with 10% CD undercompensation per span and a launched power of 0 dBm. The result is shown in Fig. 13 for different oversampling rates. Previously, BP-1S at $M/K = 3$ achieved a phase error s.d. of 0.051 rad. For BP-MS to achieve within 2 dB of the performance of BP-1S, N_{iter} must be at least 17, which is only marginally less than the 25 spans of fiber in the link. Thus, BP-MS does not result in significant computational savings.

D. Backpropagation With Subspan Step Size

One of the goals in system design is to achieve high spectral efficiency. There are two methods of fulfilling this: (i) increase the bit rate of individual channels while maintaining a fixed channel spacing; (ii) maintain a low bit rate per channel but reduce the channel spacing. These options have different system implications. A higher symbol rate will lead to greater dispersion-induced distortion, which will interact more strongly with nonlinearity over shorter distances. In Fig. 14, we plot the performance of BP-1S for 53.5 Gb/s 50% RZ-QPSK for the
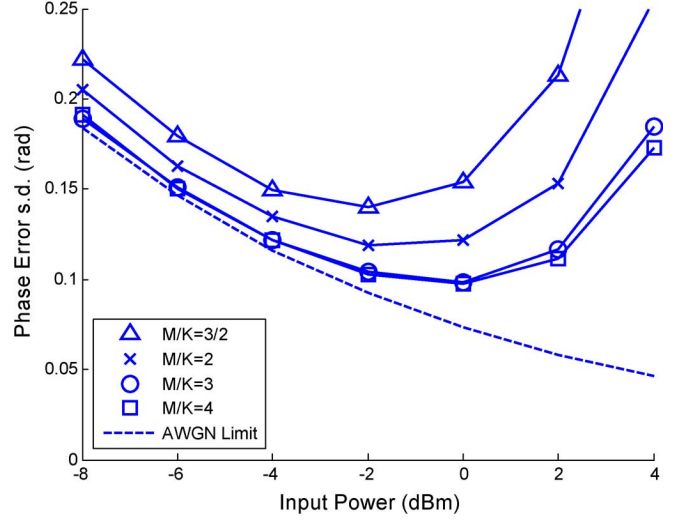
channel considered in Section II with 10% CD undercompensation per span. Compared to Fig. 9(c), we observe less performance improvement using $M/K = 3$ and 4 at 53.5 Gb/s than at 21.4 Gb/s, due to enhanced CD distortion that scales as R_s^2. In Section III-A, we noted that CD and Kerr nonlinearity are phase effects in the frequency and time domains. In order to compute the NLSE accurately using the SSFM, the linear and nonlinear phase shifts over the step size h must be small. To overcome the greater CD distortion at 50 Gb/s, a subspan step size is required. As in [14], we divide each fiber span into N_{sec} sections of equal length, with the difference that we use a noniterative asymmetric model for each step [Fig. 4(d)] where

$$H_{smf}^{(i)}(\omega) = \exp\left(-j\frac{\beta_{2,smf}L_{smf}\omega^2}{2N_{\text{sec}}}\right) \qquad (17)$$

$$H_{dcf}^{(i)}(\omega) = \exp\left(-j\frac{\beta_{2,dcf}L_{dcf}\omega^2}{2N_{\text{sec}}}\right) \qquad (18)$$

$$\xi_{NL,smf}^{(i)} = \xi\gamma_{smf}L_{\text{eff},smf}e^{-\alpha_{smf}L_{smf}(i-1)/N_{\text{sec}}} \qquad (19)$$

$$\xi_{NL,dcf}^{(i)} = \xi\gamma_{dcf}L_{\text{eff},dcf}(Ge^{-\alpha_{smf}L_{smf}})$$
$$\times e^{-\alpha_{dcf}L_{dcf}(i-1)/N_{\text{sec}}} \qquad (20)$$

and ξ is a parameter to be optimized empirically. Fig. 15 shows the performance of BP-SS for the system considered previous at $M/K = 2$, 3, and 4. As expected, the performance of BP-SS improves with increasing N_{sec}. In particular, the use of BP-SS with $N_{\text{sec}} = 6$ and $M/K = 3$ achieves 1 dB better performance than BP-1S at the same oversampling. Thus, reducing the step-size can indeed overcome enhanced CD. However, systems at 50 Gb/s also suffer from PMD for realistic transmission distances [2]. Signal propagation for systems with significant PMD needs to be modeled by a vectored NLSE [20]. In theory, the channel can be inverted using dual-polarization BP, which can be approximated by a noniterative asymmetric SSFM where the nonlinear and linear steps are described by multiplications with 2×2 matrices in the time and frequency domain. The receiver needs to know the Jones matrix of each fiber section that is backpropagated. Thus, in contrast to inverting the scalar NLSE
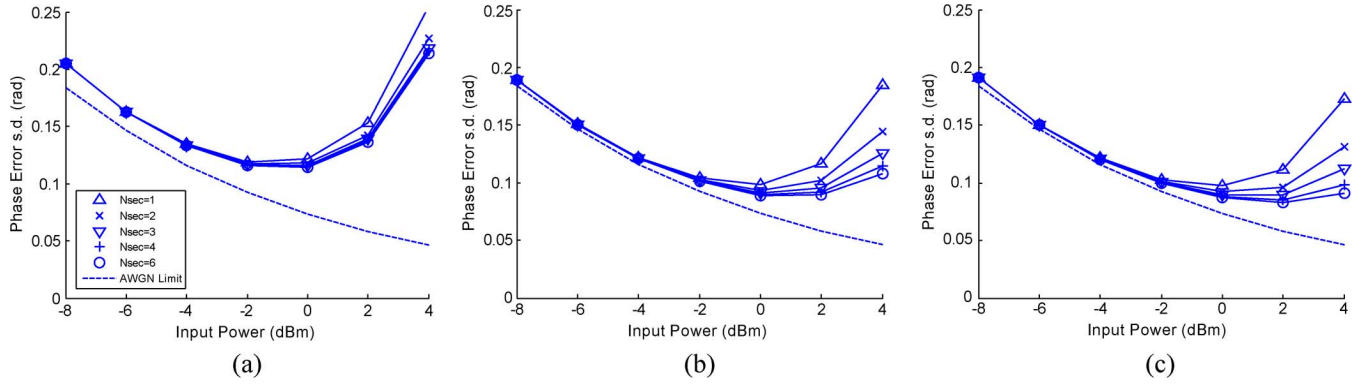
Fig. 15. Performance of BP-SS for 53.5 Gb/s 50% RZ-QPSK transmitted over 25×80 km spans of SMF with 10% CD undercompensation per span. T The oversampling rates M/K are: (a) 2; (b) 3; and (c) 4.
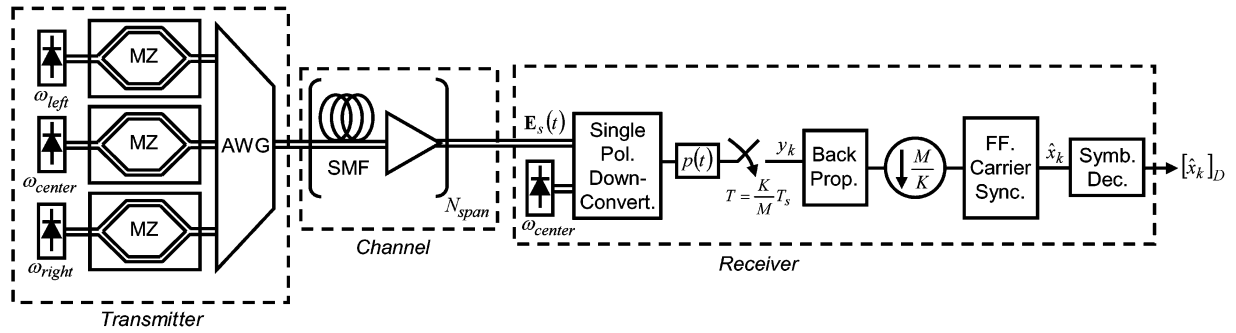

Fig. 16. Simulation of a three-channel WDM system. The input 21.4 Gb/s 50% RZ-QPSK signals are combined using an AWG whose channel bandwidths are 80% of the channel spacing.

which depends on only two parameters ($\beta_2 L$ and γL_{eff}), BP for the general vectored NLSE requires knowledge of the PSP and DGD of every fiber section. The number of time-varying parameters that need to be estimated becomes unrealistically large.

E. WDM

Since PMD is significant at symbol rates above 10 Gsymbol/s and is likely to render BP at 25 Gsymbol/s infeasible, it becomes difficult to increase spectral efficiency by holding the channel spacing at 50 GHz and increasing the symbol rate per channel. A more realistic approach to increase spectral efficiency without increasing the SNR requirement is to decrease the channel spacing, which enhances XPM. To estimate the impact of XPM on performance, we performed a three-channel simulation whose system model shown in Fig. 16. Three independent, copolarized channels modulated by 21.4 Gb/s 50% RZ-QPSK data are multiplexed using an arrayed waveguide grating (AWG). The baseband amplitude response of the AWG for each channel is assumed to be super-Gaussian: $H_{AWG}(\omega) = \exp(-0.5 \ln 2(2\omega/\omega_{1/2})^{2m})$ with $m = 1/2$ and $\omega_{1/2} = 2\pi(0.8)f_{ch}$, i.e., a 3-dB bandwidth equal to 80% of the channel spacing. We selected a launched power of 0 dBm for each channel. The WDM signal is transmitted over 25×80 km spans of SMF with inline amplification only. DCF was omitted as per Section III-B. At the receiver, the LO laser frequency is tuned to that of the center channel. The analog output of the downconverter is filtered by a Butterworth filter whose 3-dB bandwidth is equal to 40% of the sampling rate. For our simulation, we used $M/K = 3$. Fig. 17 shows the change in system performance with channel spacing. We observe that BP-1S

gives the same performance as iterative symmetric BP, while vastly outperforming linear equalization only. The reference curve labeled "AWGN + Crosstalk" denotes back-to-back performance where AWGN of the appropriate power spectral density equal to the sum of all the EDFAs was added to the transmitted signal, which was then detected without using BP. The gap between AWGN + Crosstalk and the AWGN limit is the result of linear crosstalk between channels, whereas the gap between BP and AWGN + Crosstalk is the result of nonlinear effects. System performance becomes significantly poorer when channel spacing is reduced below 25 GHz, largely due to linear crosstalk.

F. Adaptative Backpropagation

In the BP algorithms considered—even for BP-1S and BP-MS—knowledge of the fiber parameters and signal power levels is required by the receiver. Since these parameters may not be known in advance, and in reconfigurable systems, the link may be time varying, it is desirable that BP be made adaptive.

Consider single-polarization transmission with no DCF where PMD is negligible. Assuming the fiber spans are identical, BP depends on only two parameters: $\beta_2 L$ and γL_{eff}. It is possible for the receiver to perform BP using different trial values of these parameters, measuring the resulting phase error variance to determine the pair of parameters that gives the best results. Fig. 18 shows the output phase error s.d. for BP-1S when β_2 and γ are perturbed about their optimum values. The performance surface is bowl shaped. One possible adaptive algorithm is to initially set the receiver to perform
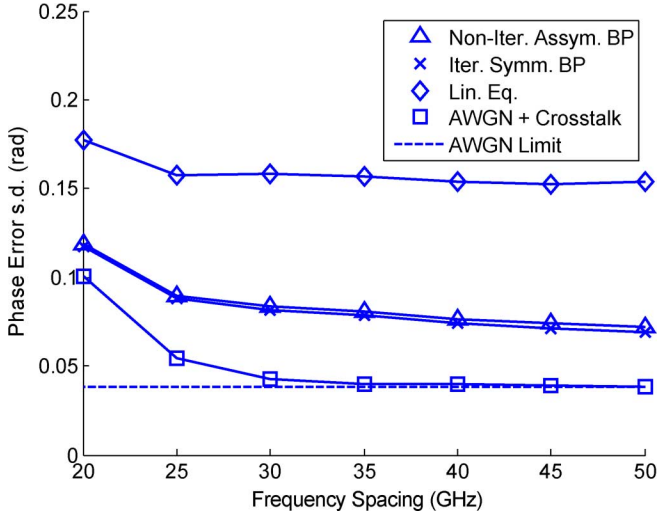
Fig. 17. System performance vs. channel spacing for a three-channel WDM system transmitted over 25 × 80 km of SMF with no DCF. Each channel transmits 50% RZ-QPSK data at 21.4 Gb/s and 0 dBm power.
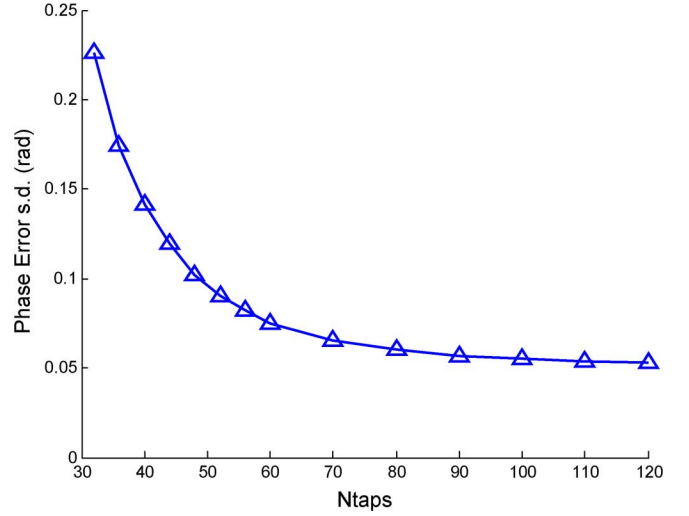

Fig. 19. Performance of BP-1S versus length of the linear filter for 21.4 Gb/s 50% RZ-QPSK transmitted over 25 × 80 km spans of SMF with no DCF. The signal launched power is 0 dBm.
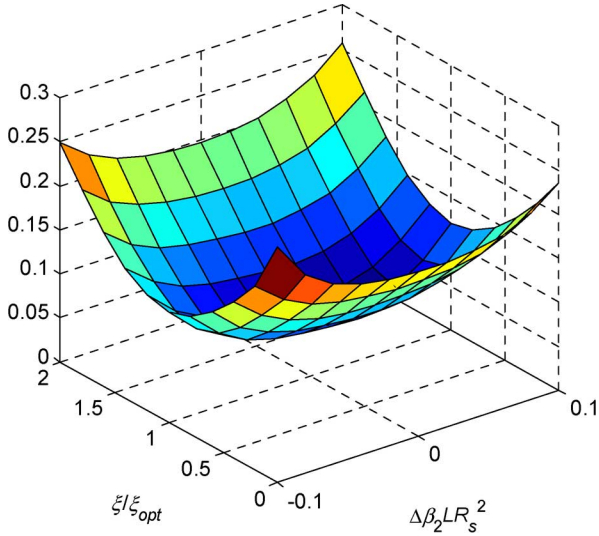

Fig. 18. Performance surface obtained for BP-1S when the linear and nonlinear parameters of the algorithm are perturbed about their optimum values. These results were obtained for single-channel 50% RZ-QPSK at 21.4 Gb/s transmitted over ×80 km of SMF with no DCF.

linear equalization only [Fig. 3(a) without the NLPN compensation section], and adapting the coefficients of the filter with a well-known algorithm like least-mean squares (LMS). The filter taps will converge to a solution that approximately inverts the dispersion of the channel. Upon taking the phase of the FFT of the filter coefficients, an estimate of the link's $\beta_2 L$ is obtained. The receiver can then begin detection using BP-1S with the linear coefficient found, and the parameter of the nonlinear stage can be adjusted until the lowest phase error s.d. is measured.

G. Computation Requirement

Finally, we compare the copmutation requirements of BP-1S and linear equalization. We consider single-channel 50% RZ-QPSK at 21.4 Gb/s transmitted over 25 × 80 km spans of SMF (no DCF) at a launched power of 0 dBm. In a real-time implementation, we replace the FFT in Fig. 8 with a linear filter of length N_{tap}. Assuming N_{tap} is even, we set the filter coefficients to

$$h_{\text{smf,comp}}(n) = \sum_{k=-N_{\text{tap}}/2}^{N_{\text{tap}}/2-1} \exp\left(j\frac{\beta_{2,smf}L_{smf}}{2}\left(\frac{2\pi k}{N_{\text{tap}}T}\right)^2\right)$$
$$\times \exp\left(-j\frac{2\pi k(n-N_{\text{tap}}/2)}{N_{\text{tap}}}\right) \text{ for } 0 \le n \le N_{\text{tap}}-1. \quad (21)$$

Fig. 19 shows the output phase error s.d. versus N_{tap}. In order to achieve performance within 2 dB of that of using an FFT with very long block length [Fig. 9(d)], 70 filter taps are required. The computation requirement is as follows: since one complex multiply is equal to four real multiplies, the linear step requires $4N_{\text{tap}}$ real multiplications. In the nonlinear step, the squared magnitude function requires two real multiplies, while multiplication by ξ_{NL} requires another multiply. The exponential function is assumed to be implemented with a lookup table. Finally, four real multiplies are required to compute the phase-rotated output. For a link with N_{span} of fiber, the total complexity is $(M/K)N_{\text{span}}(4N_{\text{tap}}+7)$ real multiplications per symbol. In the hypothetical system considered in Fig. 19, this corresponds to 21 515 real multiplications per symbol.

Conversely, it was shown in [2] that neglecting nonlinear effects, a fractionally spaced linear equalizer requires $N_{\text{tap},lineq} = 2\pi|\beta_2|N_{\text{span}}L_{smf}R_s^2(M/K)$ taps to compensate CD with low power penalty, and an oversampling rate of $M/K = 3/2$ is sufficient. For our hypothetical system, the complexity requirement is only $4N_{\text{tap},lineq} = 188$ real multiplications per symbol. An block-based FFT implementation can further reduce the computation requirement further [19]. Therefore, even with our reduced complexity algorithm based on a noniterative asymmetric SSFM, BP-1S requires >100 times more operations per symbol than linear equalization only. However, linear equalization achieves a phase error s.d. of 0.14 rad, and is almost 7 dB worse than BP-1S. When DCF is used, the impulse response duration of the channel is shortened. This

reduces the computational requirement of linear equalization still further, but not for BP.

IV. CONCLUSION

We studied receiver-based digital signal processing algorithms for the joint compensation of linear and nonlinear impairments in fiber. In long-haul terrestrial systems employing inline amplification and dispersion compenation, linear and nonlinear impairments are intertwined and cannot be compensated separately at the receiver. BP is a universal technique that enables the joint mitigation of linear and nonlinear impairments for an arbitrary channel. BP requires solving the inverse NLSE for the channel and is computationally expensive. We studied a reduced-complexity algorithm employing a noniterative asymmetric split-step Fourier method (SSFM). Our results showed that using a step size equal to the length of a fiber span is a reasonable compromise between performance and computational requirement for a symbol rate of 10 Gsymbol/s, where PMD is negligible. We found that the best system performance is obtained by omitting the use of dispersion-compensation fiber (DCF), as CD can be compensated digitally without incurring loss or nonlinear effects. For good numerical accuracy, digital BP should be performed at three-times oversampling. Using these empirical system design rules, we found that BP enables RZ-QPSK transmission over distances greater than 6400 km, whereas a receiver implementing linear equalization can transmit 2000 km only. BP is not suitable for systems with significant PMD, as it is infeasible for the receiver to estimate the Jones matrix of all fiber sections to be backpropagated. This renders BP unsuitable for transmission at 25 Gsymbol/s where PMD is nonnegligible over realistic transmission distances. To increase spectral efficiency, it is more desirable to use a lower data rate per channel with narrower channel spacing than to increase the symbol rate while keeping the channel spacing fixed at 50 GHz.

REFERENCES

[1] J. Winters, "Equalization in coherent lightwave systems using a fractionally spaced equalizer," *J. Lightw. Technol.*, vol. 8, no. 10, pp. 1487–1491, Oct. 1990.

[2] E. Ip and J. M. Kahn, "Digital equalization of chromatic dispersion and polarization mode dispersion," *J. Lightw. Technol.*, vol. 25, no. 8, pp. 2033–2043, Aug. 2007.

[3] S. J. Savory, G. Gavioli, R. I. Killey, and P. Bayvel, "Electronic compensation of chromatic dispersion using a digital coherent receiver," *Opt. Expr.*, vol. 15, no. 5, pp. 2120–2126, March 2007.

[4] M. G. Taylor, "Accurate digital phase estimation process for coherent detection using a parallel digital processor," presented at the Proc. European Conference on Optical Communication (ECOC 2005),, Glasgow, U.K., 2005, Paper Tu4.2.6, unpublished.

[5] D.-S. Ly-Gagnon, S. Tsukamoto, K. Katoh, and K. Kikuchi, "Coherent detection of optical quadrature phase-shift keying signals with carrier phase estimation," *J. Lightw. Technol.*, vol. 24, no. 1, pp. 12–21, Jan. 2006.

[6] K. Kikuchi, "Phase-diversity homodyne detection of multilevel optical modulation with digital carrier phase estimation," *IEEE J. Sel. Topics Quantum Electron.*, vol. 12, no. 4, pp. 563–570, Jul.–Aug. 2006.

[7] E. Ip and J. M. Kahn, "Feedforward carrier recovery for coherent optical communications," *J. Lightw. Technol.*, vol. 25, no. 9, pp. 2675–2692, Sep. 2007.

[8] M. Shtaif, E. Eiselt, and L. D. Garret, "Cross-phase modulation distortion measurements in multispan WDM systems," *IEEE Photon. Technol. Lett.*, vol. 12, no. 1, pp. 88–90, Jan. 2000.

[9] K. Roberts, C. Li, L. Strawczynski, M. O'Sullivan, and I. Hardcastle, "Electronic precompensation of optical nonlinearity," *IEEE Photon. Technol. Lett.*, vol. 18, no. 2, pp. 403–405, Jan. 2006.

[10] A. Chowdhury and R.-J. Essiambre, "Optical phase conjugation and pseudolinear transmission," *Opt. Lett.*, vol. 29, no. 10, pp. 1105–1107, May 2004.

[11] P. Minzioni, I. Cristani, V. Degiorgio, L. Marazzi, M. Martinelli, C. Langrock, and M. M. Fejer, "Experimental demonstration of nonlinearity and dispersion compensation in an embedded link by optical phase conjugation," *IEEE Photon. Technol. Lett.*, vol. 18, no. 9, pp. 995–997, May 2006.

[12] S. Kumar and L. Liu, "Reduction of nonlinear phase noise using optical phase conjugation in quasi-linear optical transmission," *Opt. Expr.*, vol. 15, no. 5, pp. 2166–2177, Mar. 2007.

[13] K.-P. Ho and J. M. Kahn, "Electronic compensation technique to mitigate nonlinear phase noise," *J. Lightw. Technol.*, vol. 22, no. 3, pp. 779–783, Mar. 2004.

[14] X. Li, X. Chen, G. Goldfarb, E. Mateo, I. Kim, F. Yaman, and G. Li, "Electronic post-compensation of WDM transmission impairments using coherent detection and digital signal processing," *Opt. Expr.*, vol. 16, no. 2, pp. 881–888, Jan. 2008.

[15] W. Shieh, H. Bao, and Y. Tang, "Coherent optical OFDM: Theory and design," *Opt. Expr.*, vol. 16, no. 2, pp. 841–859, Jan. 2008.

[16] K. Kikuchi, M. Fukase, and S. Kim, "Electronic post-compensation for nonlinear phase noise in a 1000-km 20-Gb/s optical QPSK transmission system using the homodyne receiver with digital signal processing," presented at the Proc. Opt. Fiber Commun. Conf. (OFC' 07), Los Angeles, CA, 2007, Paper OTuA2, unpublished.

[17] G. Charlet, N. Maaref, J. Renaudier, H. Mardoyan, P. Tran, and S. Bigo, "Transmission of 40 Gb/s QPSK with coherent detection over ultra-long distance improved by nonlinearity mitigation," presented at the Proc. European Conference on Optical Communication (ECOC 2006), Cannes, France, 2006, Paper Th4.3.4, unpublished.

[18] A. P. T. Lau and J. M. Kahn, "Signal design and detection in presence of nonlinear phase noise," *J. Lightw. Technol.*, vol. 25, no. 10, pp. 3008–3016, Oct. 2007.

[19] E. Ip, A. P. T. Lau, D. J. Barros, and J. M. Kahn, "Coherent detection in optical fiber systems," *Opt. Expr.*, vol. 16, no. 2, pp. 753–791, Jan. 2008.

[20] G. P. Agrawal, *Nonlinear Fiber Optics*, 2nd ed. London, U.K.: Academic, 1995.

[21] X. Liu and D. A. Fishman, "A fast and reliable algorithm for electronic preequalization of SPM and chromatic dispersion," presented at the Proc. Opt. Fiber Commun. Conf. (OFC' 06), Los Angeles, CA, 2006, Paper OThD4, unpublished.

[22] O. Sinkin, R. Holzlöhner, J. Zweck, and C. Menyuk, "Optimization of the split-step Fourier method in modeling optical-fiber communications systems," *J. Lightw. Technol.*, vol. 21, no. 1, pp. 61–68, 2003.

Ezra Ip received the B.E. (Hons.) degree in electrical and electronics engineering from the University of Canterbury in 2002, and the M.S. degree in electrical engineering from Stanford University, Standord, CA, in 2004. He is currently pursuing the Ph.D. degree in electrical engineering at Stanford University.

In 2002, he was a Research Engineer with Industrial Research Ltd., New Zealand. His research interests include single-mode optical fiber communications, free-space optical communications, and nonlinear optics.

Joseph M. Kahn (M'90–SM'98–F'00) received the A.B., M.A., and Ph.D. degrees in physics from the University of California (UC), Berkeley, in 1981, 1983, and 1986, respectively.

From 1987 to 1990, he was with AT&T Bell Laboratories, Crawford Hill Laboratory, Holmdel, NJ. He demonstrated multi-Gb/s coherent optical fiber transmission systems, setting world records for receiver sensitivity. From 1990 to 2003, he was with the Department of Electrical Engineering and Computer Sciences at UC Berkeley, performing research on optical and wireless communications. In 2000, he helped found StrataLight Communications, where he served as Chief Scientist from 2000 to 2003. Since 2003, he has been a Professor of Electrical Engineering with Stanford University. His current research interests include single- and multimode optical fiber communications, free-space optical communications, and MEMS for optical communications.

Prof. Kahn received the National Science Foundation Presidential Young Investigator Award in 1991. From 1993 to 2000, he served as a Technical Editor of *IEEE Personal Communications Magazine*.